Bull. Mater. Sci. (2020) 43:80
https://doi.org/10.1007/s12034-020-2046-3

Substitution tuned electronic absorption, charge transfer and non-linear optical properties of some D–A type 2,4,6-trisubstituted-1,3,5-triazines: a DFT study

V M VIDYA and CHETTI PRABHAKAR*
Department of Chemistry, National Institute of Technology, Kurukshetra 136119, India
*Author for correspondence (chetty_prabhakar@yahoo.com)

MS received 24 July 2019; accepted 19 November 2019

Abstract. We have investigated theoretically a series of donor–acceptor (D–A) type star-shaped triazine derivatives by employing density functional theory using 6-311G(d,p) basis set to understand the effect of variable substitution (on triazine core with substituents having diverse electron releasing or withdrawing capabilities) on their linear and non-linear optical properties (first hyperpolarizabilities). The investigation of influence of various electron donors/acceptors on the charge transfer characteristics of triazine molecules under study was also conducted. Present computational study reveals that the substitution of strong electron donors and greater charge delocalization enhance the first hyperpolarizability of the molecules.

Keywords. D–A star-shaped triazine; strong donor/acceptor; electronic excitations; charge transfer; first hyperpolarizability.

1. Introduction

Over the past three decades, there is growing research interest in the design, study and applications of opto-electronic materials due to their wide applications in telecommunications and optical data storage [1–6]. They are good transporters of charge as well as excellent candidates for constructing light-absorption materials in organic solar cells (OSCs) and emitters in organic light emitting diodes (OLEDs) [7–11]. Recent years have witnessed increasing popularity of triazine derivatives in area of material chemistry, whose molecular symmetry [12–15] and electronic properties [16,17] pronounce their importance in applied optoelectronics.

Recently, 1,3,5-triazines are explored to build C_3-symmetry molecules [18]. A large number of derivatives of cyanuric chloride (2,4,6-trichloro-1,3,5-triazine) have been synthesized [19–23] based on the tendency of cyanuric chloride to undergo nucleophilic substitution, where the replacement of chlorine atoms by nucleophiles is temperature-dependant. Such flexibility and versatility of nucleophilic substitution on 1,3,5-triazine core has been utilized in the construction of dendrimers [24,25]. The applications of 1,3,5-triazines are extensively researched in material science in terms of covalent triazine-based frameworks [26], as ligands in molecular organic framework (MOF) materials [27], in building caged structures for guest encapsulation [28] and in the design of single-molecule fluorescent probes [29]. Triazines have practical applications in analytical chemistry as well [30]. The donor–acceptor (D–A) type star-shaped, octupolar organic molecules with a central triazine ring, which are functionalized with multiple functional groups having varying electron donating or withdrawing ability are under intense study to explore their potential in organic electronics as donor materials in OSCs and organic field effect transistors (OFETs) [31].

The realization of triazine derivatives in the design of non-linear optical (NLO) materials has gained attention in the last few years because of asymmetric distribution of electronic charge within conjugated push–pull molecular framework of triazines. Oudar's [32–34] two-state model provides an understanding of the non-linear nature of organic molecules, having enhanced hyperpolarizabilities, expressing the dependence of first hyperpolarizability (β) on the charge transfer dipole moment ($\Delta\mu_{ge}$), square of the transition dipole moment (μ_{eg}) and the highest occupied molecular orbital–lowest unoccupied molecular orbital (HOMO–LUMO) gap (E_{ge}) [35] as in equation (1) [36].

$$\beta \propto \frac{(\mu_{ge})^2 \Delta\mu_{ge}}{(E_{ge})^2}. \tag{1}$$

It has been known that increasing the strength of the donor and complete delocalization of ground and excited states in

Electronic supplementary material: The online version of this article (https://doi.org/10.1007/s12034-020-2046-3) contains supplementary material, which is available to authorized users.

Published online: 21 February 2020

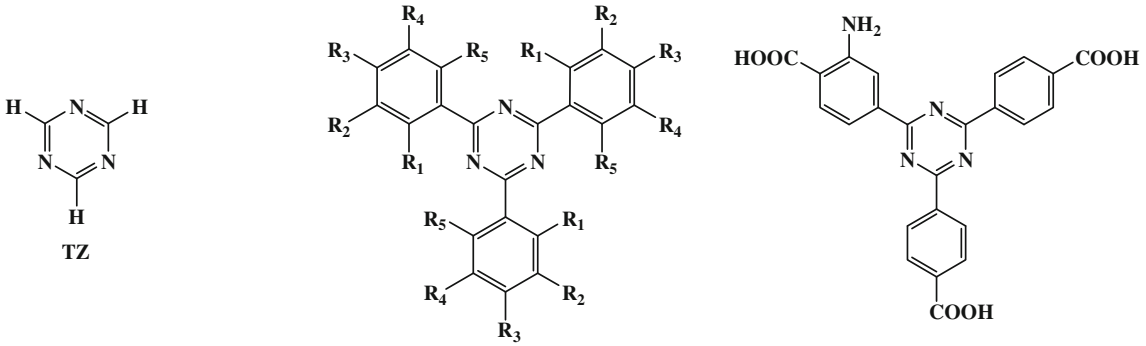

Scheme 1. TZ, unsubstituted triazine; TZ1 to TZ11, 2,4,6-trisubstituted-1,3,5-triazine; and TZ12, 2-amino-4-[4,6-bis(4-carboxyphenyl)-1,3,5-triazin-2-yl]-benzoic acid.

the octupolar molecules affect the first hyperpolarizability greatly. The influence of the multipolar transitions and transitions involving the other excited states was also investigated [37,38].

Gyoosoon and Bong [39] have studied the first hyperpolarizabilities of some triazine molecules by *ab-initio* method (Hartree–Fock level using 6-31G basis set) and showed that the first hyperpolarizability increases with the increasing donor strength of the substituents and strong donors promote greater delocalization of electronic charge. Zhu and Wu [40] have also studied a series of triazine derivatives by the coupled perturbed Hartree–Fock (CPHF) method using the 6-31G basis set and concluded that inclusion of donors into triazines favours charge transfer and therefore, increases NLO response.

Encouraged by the results of these studies [39,40], we contributed to the current knowledge by substituting the triazine core with novel groups having divergent electronic properties and by evaluating the effect of varied substitution on the linear and non-linear optical properties of the triazines. Scheme 1 shows the molecules under study from TZ to TZ12 with diverse substitutions. The unsymmetrically substituted molecule TZ12 is experimentally known [41] and is chosen to study the effect of presence of a single donor group ($-NH_2$) on one of the aromatic fragment of triazine core, when all three aromatic fragments bear electron withdrawing group (–COOH). The present study includes description of electronic excitations, frontier molecular orbitals (FMOs), charge transfer and first hyperpolarizabilities of molecules from TZ to TZ12.

2. Methodology

Previous years have seen tremendous interest of computational chemists in calculating properties of molecules using density functional theory (DFT) methods because of well agreement of theoretical results with the experimental ones. DFT calculations of the molecules TZ to TZ12 are initiated by ground state geometry optimization employing hybrid functional B3LYP [42,43] in gas phase, which combines Becke's three parameter exchange functional (B3) with the nonlocal correlation functional by Lee, Yang and Parr (LYP), with 6-311G(d, p) basis set and all the calculations are performed with the help of Gaussian 09W package [44]. For the molecules, no symmetric restrictions are imposed during the energy minimization process. Validation of molecular structures is confirmed by the existence of a local minima on potential energy surface having non-imaginary vibrational frequencies.

The calculated geometrical parameters of selected molecules TZ1, TZ2 and TZ7 were compared with their experimental crystallographic data to observe good agreement between experimental and theoretical results (supplementary tables S1–S3).

Further, we also optimized three selected molecules [TZ: unsubstituted triazine, TZ5: triazine derivative bearing electron donating ($-NH_2$) group and TZ11: triazine derivative bearing electron withdrawing ($-NO_2$) group] with different basis sets *viz*. 6-311G(d, p), 6-311+G(d, p) and 6-311++G (d, p). It is found that the effect of basis set on geometry of these selected molecules is minimum and hence, to curtail the time of computations, the basis set 6-311G(d, p) was employed for all the calculations. Comparison of computed values obtained with these three basis sets are provided in supplementary tables S4–S6.

The absorption properties and first hyperpolarizability of all the molecules are calculated by B3LYP, CAM-B3LYP, M062X, LC-WPBE, BHandHLYP and WB97XD functionals using 6-311G(d, p) basis set (absorption properties and first hyperpolarizabilities are shown in supplementary tables S7 and S8, respectively). Further, the effect of basis sets

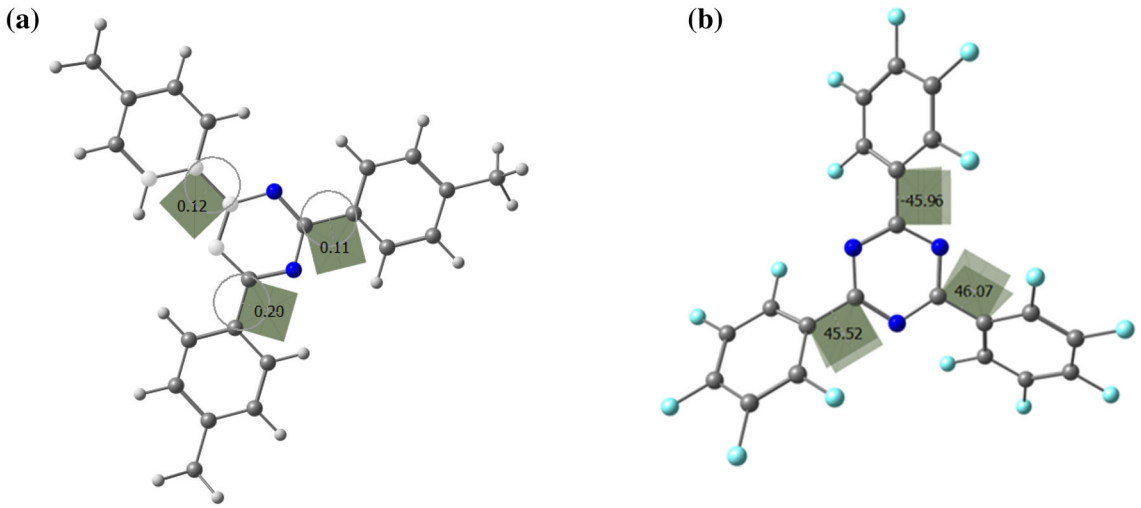

Figure 1. Structure of the molecules optimized at B3LYP/6-311G (d, p) level. (**a**) Planar molecule TZ2. (**b**) Non-planar molecule TZ10.

(6-311G(d, p), 6-311+G(d, p) and 6-311++G(d, p)) on absorption maxima of selected molecules TZ, TZ1, TZ5 and TZ11 is found to be minimum as calculated using CAM-B3LYP functional (supplementary table S9).

The first hyperpolarizabilities (β) of all the molecules under study are probed by CPHF method [45,46] using CAM-B3LYP functional. The effect of different basis sets (6-311G (d, p), 6-311+G(d, p) and 6-311++G(d, p)) on β of selected molecules TZ, TZ1, TZ5 and TZ11 is also studied and the results are provided in supplementary table S9 (discussed in section 3.5b).

3. Results and discussion

3.1 *Structure and geometry*

The structures and geometries of the molecules from TZ to TZ12 are studied using B3LYP functional with 6-311G(d, p) basis set. The carbons involved in C–C bond between central triazine core and the substituted phenyl group are sp^2 hybridized and hence, one can expect planarity in all the molecules. The phenyl rings attached to triazine core remain almost in plane (dihedral angle between substituted phenyl groups and central triazine core is $<2.5°$) with the triazine core except in the molecule TZ10. It shows that varied substitution on phenyl rings has negligible effect on the planarity of the molecule in all the molecules (except TZ10).

In case of TZ10, the high electron density on each fluorine atom substituted on one phenyl ring has repelled that on a neighbouring fluorine atom substituted on the other phenyl ring and hence became non-planar with the central triazine core, making a dihedral angle of ~45 to 46°. Structure of a representative planar molecule (TZ2) and the non-planar molecule (TZ10) are shown in figure 1.

The differential orientation of substituents ($-OCH_3$ and $-NHCOCH_3$) on phenyl ring has given rise to different configurations in the molecules TZ4 and TZ6. The molecules TZ4 and TZ6 show three configurations each, which are depicted in figure 2a and b, respectively, along with their relative energies.

3.2 *Electronic transitions and absorption spectra*

3.2a *Effect of functionals*: In general, long range functionals like CAM-B3LYP, WB97XD and LC-WPBE envisage the properties of extended π-conjugated systems to a considerably good extent. Hence, the effect of functionals on absorption properties was investigated by using B3LYP, CAM-B3LYP, M062X, LC-WPBE, WB97XD and BHandHLYP functionals using 6-311G(d, p) basis set in gas phase, which were applied on B3LYP/6-311G(d, p) optimized molecular geometries in gas phase. B3LYP hybrid functional has a constant HF (Hartree–Fock) exchange of 25% [42,43]. CAM-B3LYP (Coulomb-attenuated version of B3LYP) and WB97XD are the range separated functionals having short range of HF exchange [47]. WB97XD holds 100 and 65% HF exchanges at long and short ranges, respectively [48]. CAM-B3LYP operates at short and long range with 19 and 65% HF exchanges, respectively [47]. M062X is the global hybrid functional with 54% HF exchange [49]. LC-WPBE is the functional, which has long-range corrected version of WPBE [50]. The functional BHandHLYP provides good combination of the correctly mixed HF and LSDA (local spin density approximation) exchanges and suitable LYP correlation [51].

From the absorption maxima obtained from all the above mentioned functionals (supplementary table S7), it can be noticed that similar trends of variations of absorption maxima

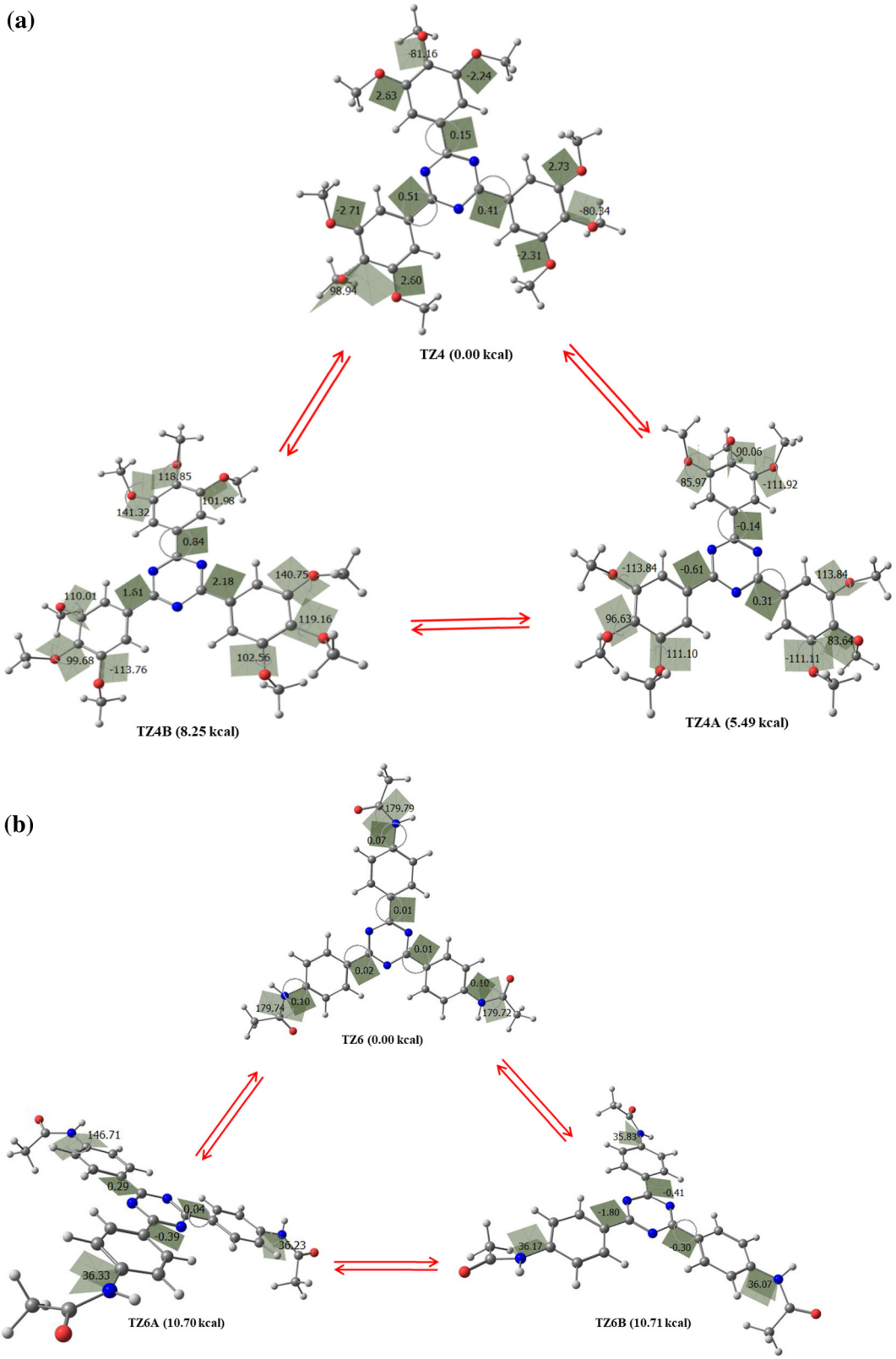

Figure 2. The configurations of (**a**) TZ4 as calculated at B3LYP/6-311G(d, p) level and (**b**) TZ6 as calculated at B3LYP/6-311G(d, p) level.

from one molecule to another is observed in each functional. B3LYP functional overestimates the absorption maxima as compared to experimental ones. Though M062X, BHandHLYP, LC-WPBE and WB97XD also predict the absorption properties reasonably; CAM-B3LYP/6-311G(d, p) obtained absorption maxima are very close the experimental absorption maxima of molecules TZ, TZ1, TZ2, TZ3, TZ4 and TZ7 [52] within the limit.

3.2b *Effect of basis sets*: It is observed that various basis sets like 6-311G(d, p), 6-311+G(d, p) and 6-311++G(d, p) do not affect absorption properties of molecules to a big extent by considering the examples of TZ, TZ1, TZ5 and TZ11 (supplementary table S9) and hence, the subsequent discussion on absorption properties follows the results obtained by CAM-B3LYP/6-311G(d, p) method.

The calculations of wavelength of maximum absorption (λ_{cal}) and experimental absorption maxima (λ_{exp}) [52] are compared in table 1. Selected electronic excitations, oscillator strength (f) and mixing coefficients ($\%C_i$) of all the molecules under study are also shown in table 1.

The experimental absorption maxima for molecule TZ is 260 nm [52], which is in accordance with calculated absorption maxima of 255 nm which arises due to major transitions from HOMO-1 → LUMO and HOMO → LUMO+1.

The TZ1 and TZ2 molecules, which have three phenyl and three p-tolyl groups substituted on central triazine core (TRZ), respectively, show low intensity absorption maxima at 267 and 266 nm, respectively, which are redshifted from TZ by 12 and 11 nm, respectively, due to extension of pi-conjugation. The TZ1 and TZ2 molecules also absorb in high intensities at 254 and 267 nm, respectively, in second excited state (S2) as shown in table 1.

As the electron donating capacity of substituents increase in molecules in the order of TZ3 < TZ4 < TZ6 < TZ5 as compared to TZ; one can notice that red shifting of absorption maxima from TZ is also increasing. From table 1, we can see the redshift of TZ3, TZ4, TZ5 and TZ6 by 19, 26, 29 and 29 nm, respectively, as compared to TZ. The moderately electron donating –Cl group bearing molecule TZ7 shows a low intensity excitation at 267 nm and exhibits a lesser redshift of 12 nm from TZ as compared to red shift caused by strong donors. It also shows high intensity absorption maxima at 264 nm in second excited state.

The increasing electron withdrawing effect of substituents in molecules TZ8, TZ9, TZ10 and TZ11, results in lowered value of absorption maxima as compared to strong donor-bearing molecules like TZ5. The TZ8 and TZ9 molecules absorb both at low and high intensities as indicated in table 1. The TZ11 molecule bearing strong electron withdrawing $-NO_2$ absorbs at low intensities.

In general, the absorption maxima with higher oscillator strengths have greater intensity and hence are believed to be arising because of π → π* electronic transitions. The TZ12 molecule shows two bands in UV absorption spectra. One absorption band of longer wavelength (LW) shows absorption maxima at 354 nm ($f = 0.103$), which is attributed to π → π* transition within the heterocyclic moiety formed due to intramolecular hydrogen bonding between –COOH and $-NH_2$ at o-position to each other. The second absorption band of shorter wavelength (SW) indicates its absorption maxima at 265 nm ($f = 0.353$), which is again attributed to π → π* transition within the benzenoid system as in the case of 2-aminobenzoic acid [53].

The optoelectronics of the molecules can be comprehended by studying the energy of the highest occupied molecular orbital (E_{HOMO}), the energy of the lowest unoccupied molecular orbital (E_{LUMO}) and the HOMO–LUMO gap (E_g) of the molecules. Table 2 enlists E_{HOMO}, E_{LUMO} and E_g of the molecules from TZ to TZ12. The trend of variation of energies of HOMO and LUMO levels of representative molecules TZ, TZ3, TZ5, TZ7, TZ9 and TZ11 is presented in figure 3, which indicates that both HOMO and LUMO show increasing destabilization as donor strength of substituents increases and increasing stabilization as electron-withdrawing power of substituents increases.

The molecules show varying E_g values because of the varying magnitudes of destabilization and stabilization (affected by differing electronic nature of substituents) of FMOs as compared to other molecules. The HOMO of TZ3 and TZ5 are destabilized by 1.64 and 2.16 eV, respectively, as compared to that of TZ, while LUMO of TZ3 and TZ5 are destabilized by 0.12 and 0.42 eV as compared to that of TZ. In the case of TZ3 and TZ5, the destabilization of HOMO levels occurs in higher magnitudes than that of LUMO levels and hence, the band gap goes on narrowing as we move from TZ to TZ3 to TZ5.

The TZ7, TZ9 and TZ11 molecules have moderate electron-withdrawing –Cl group, strong electron-withdrawing $-CF_3$ and $-NO_2$ groups, respectively, and hence, cause removal of electron density from HOMO and make them stable as electron-withdrawing capacity increases in the order $-Cl < -CF_3 < -NO_2$. The HOMOs of TZ7, TZ9 and TZ11 attain stability at 1.50, 2.09 and 2.51 eV, respectively, as compared to that of TZ5, which has strong electron-donating $-NH_2$ functional group. Meanwhile, the LUMO levels of TZ7, TZ9 and TZ11 get stabilized by 1.14, 1.51 and 2.22 eV, respectively, as compared to that of TZ5.

These results clearly point out the fact that energies of FMOs and band gaps are profoundly impacted by substitution of different functional groups with diverse electronic properties. The E_g values of molecules under examination follow the order: TZ12 < TZ6 < TZ5 < TZ4 < TZ3 < TZ11 < TZ7 < TZ2 < TZ10 < TZ9 < TZ1 < TZ and the reverse order follows for absorption maxima in scale. The molecule TZ with largest HOMO–LUMO gap has shortest wavelength of maximum absorption as confirmed both theoretically and experimentally. The molecule TZ12 having shortest HOMO–LUMO gap shows the longest wavelength of maximum absorption.

Table 1. The experimental absorption maxima (λ_{exp} in nm) measured in THF, theoretical absorption maxima in gas phase (λ_{cal} in nm), theoretical absorption maxima in solvent THF (λ_{thf} in nm), oscillator strength (f), major electronic transitions (MT) and mixing coefficient ($\%C_i$) of the molecules under study calculated at CAM-B3LYP/6-311G(d, p) level of theory.

Name	λ_{exp}	Calculated absorption maxima		f	MT	$\%C_i$
		Excited state	λ_{cal} (λ_{thf})			
TZ	260	S1	255 (251)	0.016	H-1 → L	48
					H → L + 1	45
TZ1	265	S1	267 (266)	0.005	H-7 → L	47
					H-6 → L + 1	46
		S2	254 (259)	0.625	H-2 → L + 1	29
					H → L + 1	18
					H-1 → L	18
TZ2	284	S1	266 (268)	0.006	H-7 → L + 1	25
					H-6 → L	25
					H-7 → L	21
					H-6 → L + 1	21
		S2	267	0.9587	H-1 → L + 1	28
					H → L	28
					H-2 → L + 1	25
TZ3	300	S1	274 (282)	1.054	H-2 → L	35
					H-1 → L + 1	26
					H → L	26
TZ4	314	S1	281 (284)	0.056	H → L + 1	49
					H-1 → L	11
TZ5	—	S1	284 (297)	1.071	H-2 → L	28
					H-1 → L	18
					H → L + 1	17
					H-1 → L + 1	9
TZ6	—	S1	284 (292)	1.331	H-2 → L	29
					H → L	25
					H-1 → L + 1	25
					H-2 → L + 1	7
TZ7	278	S1	267 (268)	0.005	H-6 → L	36
					H-5 → L + 1	36
					H-7 → L + 1	10
					H-6 → L	10
		S2	264 (269)	1.0232	H-2 → L	30
					H-1 → L + 1	25
					H → L	24
TZ8	—	S1	273 (270)	0.005	H-7 → L + 1	28
					H-6 → L	27
					H-6 → L + 1	17
					H-7 → L	17
		S2	268 (271)	1.0784	H-2 → L	32
					H-1 → L	20
					H → L + 1	19
TZ9	—	S1	270 (271)	0.006	H-7 → L	45
					H-6 → L + 1	44
		S2	255 (257)	0.366	H → L	15
					H-2 → L	10
					H-1 → L + 1	15
					H-2 → L + 1	10
TZ10	—	S1	271 (268)	0.010	H-6 → L	44
					H-7 → L + 1	41
TZ11	—	S1	283 (278)	0.001	H-14 → L + 1	27
					H-16 → L	14
					H-15 → L + 1	13

Table 1. (continued)

Name	λ_{exp}	Calculated absorption maxima				
		Excited state	λ_{cal} (λ_{thf})	f	MT	$\%C_i$
		S2	274 (278)	0.005	H-6 → L + 1	19
					H-7 → L	19
					H-7 → L + 1	17
					H-6 → L	16
TZ12	—	S1	354 (359)	0.103	H → L + 1	73
		S2	265 (267)	0.353	H-1 → L + 1	29
					H-4 → L	13
					H-2 → L	12
					H-3 → L + 1	11

Table 2. Energies of HOMO (E_{HOMO} in eV), LUMO (E_{LUMO} in eV) and HOMO–LUMO energy gap (E_g in eV) of the molecules from TZ to TZ12 calculated at B3LYP/6-311G(d, p) level.

Name	E_{HOMO}	E_{LUMO}	E_g
TZ	−7.74	−1.77	5.97
TZ1	−6.90	−2.06	4.84
TZ2	−6.59	−1.88	4.71
TZ3	−6.10	−1.65	4.45
TZ4	−6.01	−1.92	4.09
TZ5	−5.58	−1.34	4.24
TZ6	−6.22	−1.90	4.32
TZ7	−7.08	−2.48	4.60
TZ8	−7.75	−3.24	4.51
TZ9	−7.67	−2.85	4.82
TZ10	−7.65	−2.90	4.75
TZ11	−8.09	−3.56	4.53
TZ12	−5.99	−2.74	3.25

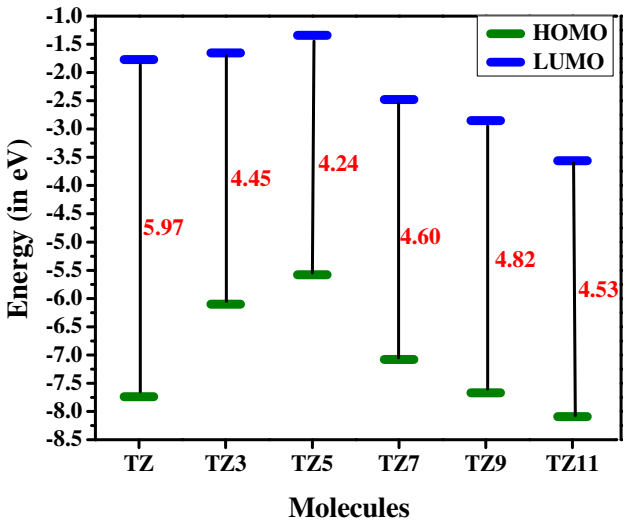

Figure 3. Comparison of energies of HOMO and LUMO levels (in eV) and energy gap (in eV) of selected molecules TZ, TZ3, TZ5, TZ7, TZ9 and TZ11 calculated at B3LYP/6-311G(d, p) level.

3.3 *FMOs*

The FMOs comprising of the HOMO and LUMO of the molecules under study from TZ to TZ12 are visualized based on CAM-B3LYP/6-311G (d, p) level of theory. The FMOs of representative molecules TZ4 and TZ12 along with major electronic transitions occurring in them are shown in figure 4. The HOMO and LUMO of each of molecules TZ, TZ1, TZ2, TZ3, TZ5, TZ6, TZ7, TZ8, TZ9, TZ10 and TZ11 are provided in supplementary figure S1.

The electron density is majorly located on nitrogen atoms of 1,3,5-triazine core in HOMO of TZ. In LUMO of TZ, electron density gets shifted on carbon atoms of the triazine ring in high magnitudes. Unsymmetrical charge distribution in HOMO and LUMO becomes clearly visible in star-shaped D–A type of molecules, when TZ is substituted with groups of varying electron donating/accepting ability as in the molecules from TZ1 to TZ12.

The molecules TZ1 to TZ4 bear three arms of electron-donating aromatic groups (AR) on the central triazine (TRZ) moiety. AR fragments have major contribution to the HOMO of these molecules with minor contributions from the TRZ. In TZ1 and TZ2, HOMO levels are localized mainly on one AR with moderate charge on rest two AR and TRZ ring. LUMO of TZ1 shows concentration of charge density on TRZ and two AR fragments. Hence, here TRZ acts as acceptor with one AR fragment being major donor.

TZ3 shows high electron density on two AR fragments in HOMO, which act as donor and the TRZ being acceptor in LUMO. HOMO of TZ4 is mainly located on two AR fragments making them electron donors and the other one AR and TRZ being acceptors in LUMO. It can be noticed that there is minor charge density on methoxy groups on AR fragments in both HOMO and LUMO of TZ3 and TZ4.

The molecules TZ5 and TZ6 have AR fragments with electron-donating amine functionality on it. HOMO of TZ5 obtains major contribution from two AR fragments, which act as donors and the acceptor being triazine core. TZ6 also

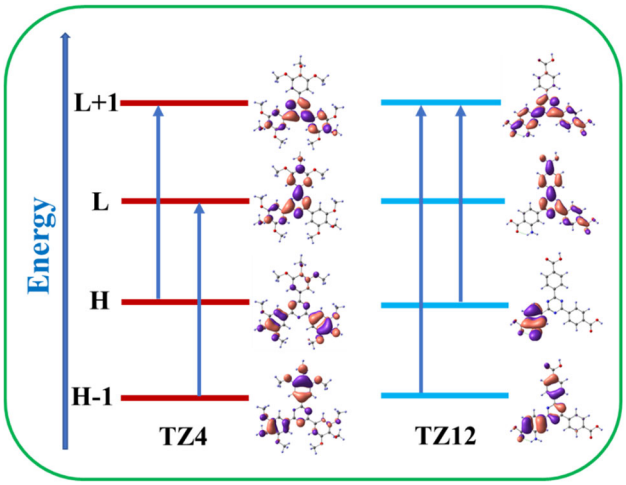

Figure 4. Schematic representation of the frontier molecular orbitals and major electronic transitions of TZ4 and TZ12 calculated at CAM-B3LYP/6-311G(d, p) level of theory.

follows this trend of electron-density distribution in its HOMO and LUMO. In TZ6, major donors are two AR fragments and the major acceptor is the TRZ ring. In molecule TZ7, two AR fragments donate electron density to TRZ core and third AR fragment. One AR fragment remains inactive in charge transfer from HOMO to LUMO in molecule TZ8. The two AR fragments contain the major electron density in HOMO of TZ8, while electron density has been moderately shifted to TRZ core from two AR fragments (due to electron withdrawing nature of –CN functionality).

In TZ9, charge transfer takes place majorly from one AR fragment (donor) and minorly from second AR fragment. This donated charge shifts to third AR fragment in minor amounts and TRZ moiety in major amounts. The molecule TZ10 has its charge density concentrated mainly on one of the AR fragment in HOMO, which transfers charge density to two other AR fragments and TRZ core in LUMO.

The molecules TZ11 and TZ12 bear strong electron-withdrawing groups in AR fragments, which show remarkable intramolecular charge transfer from HOMO to LUMO. The HOMO of TZ11 molecule has charge distributed all over the molecule and charge flows into two AR fragments and TRZ in LUMO. In TZ12, charge is greatly localized on only one AR fragment bearing both $-NH_2$ and –COOH groups in HOMO, which transfers its electron density to other two AR fragments and TRZ in LUMO.

3.4 *Charge transfer*

Charge transfer (CT) is influenced by the electron donor or acceptor strength [54,55]. The incorporation of various donor or acceptor groups enhances CT in triazine derivatives. We carried out CT studies using VModes software [56] and the

Table 3. CT (in electron units) from ground state to excited state of molecules TZ1 to TZ12 calculated at B3LYP/6-311G(d, p) level.

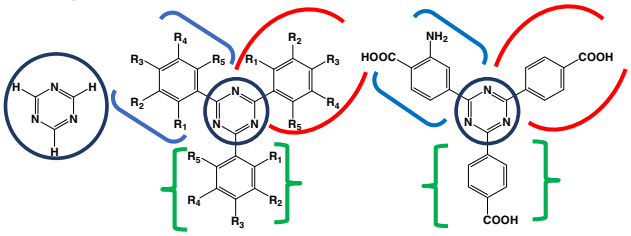

Name	Group I (O)			Group II ([])			Group III (())			Group IV({})		
	H	L	D[a]	H	L	D[a]	H	L	D[a]	H	L	D[a]
TZ1	25.9	57.4	31.5	18.8	25.0	6.2	43.5	3.5	−40.0	11.8	14.1	2.3
TZ2	9.8	55.4	45.6	40.4	4.1	−36.3	23.7	8.4	−15.3	26.1	32.0	5.9
TZ3	17.6	39.0	21.4	4.9	33.7	28.8	34.0	15.4	−18.6	43.5	11.9	−31.6
TZ4	3.7	52.7	49.0	41.0	2.8	−38.2	30.4	12.1	−18.3	24.2	29.6	5.4
TZ5	2.4	42.5	40.1	34.6	26.9	−7.7	33.3	15.4	−17.9	29.6	15.2	−14.4
TZ6	5.6	34.9	29.3	40.5	34.2	−6.3	38.9	16.8	−22.1	15.0	14.1	−0.9
TZ7	7.0	52.7	45.7	49.9	5.8	−44.1	31.2	8.3	−22.9	12.0	33.3	21.3
TZ8	15.1	36.0	20.9	31.0	31.2	0.2	29.1	20.5	−8.6	24.9	12.4	−12.5
TZ9	9.7	36.4	26.7	39.6	34.8	−4.8	27.6	16.6	−11	23.1	12.3	−10.8
TZ10	0.6	46.8	46.2	5.1	26.6	21.5	32.8	13.1	−19.7	61.5	13.5	−48
TZ11	0.4	45.1	44.7	75.6	9.6	−66	23.8	14.4	−9.4	0.1	30.9	30.8
TZ12	19.1	32.8	13.7	16.3	21.1	4.8	25.4	15.2	−10.2	39.2	30.9	−8.3

[a]D is the loss/gain of charge. Positive value of D indicates that the corresponding group behaves as the electron acceptor, while negative value indicates charge donation by the respective group.

results are shown in table 3, depicting the distribution of electron density in HOMO (H) and LUMO (L) of molecules from TZ1 to TZ12, each of which is subdivided into four groups: group I (central triazine core), group II, group III and group IV (substituents on central triazine core). The molecule TZ is excluded, since it does not have any substituents.

The central triazine ring in all the molecules is considered as group I and the three AR fragments substituted on triazine are considered as group II, III and IV. The results displayed in table 3 suggest that the triazine core acts as an acceptor, since the contributions of the AR fragments to LUMO levels are increased. Table 3 also shows the influence of substitution on CT in the molecules under study.

Considering the molecule TZ1, which has three phenyl groups as its three AR fragments, it can be observed that group I acts as a charge acceptor by accepting the charge of 31.5 e from group III, which donates a charge of 40 e.

In TZ2 molecule, the three AR fragments are substituted with electron-donating $-CH_3$ group, which enhances the electron acceptance of group I by 14.1 e, pulling the charge from groups II and III. The molecule TZ5, having electron-donating $-NH_2$ group on its all three AR fragments, has the electron acceptance of group I increased by 8.6 e compared to the unsubstituted TZ1 molecule, while charge flows from groups II, III and IV.

The TZ4, TZ7 and TZ10 molecules having the electronegative atoms (–O, –Cl and –F, respectively) attached to the phenyl ring in AR fragments, also show charge donation by a positive mesomeric effect. This can be observed in the raise of electron acceptance of group I by 17.5, 14.2 and 14.7 e in the molecules TZ4, TZ7 and TZ10, respectively, as compared to TZ1. Similarly, the negative inductive effect of substituents in the molecules TZ3, TZ6, TZ8 and TZ9 have reduced the charge flow into group I as compared to TZ1.

The molecule TZ11 is substituted with strong electron-withdrawing group $–NO_2$ on all the AR fragments, due to which the flow of electrons is diminished into the group I, reducing its electron-accepting ability by 17.8 e as compared to TZ1.

The TZ12 molecule bears strong electron-withdrawing–COOH groups on its all three AR fragments also show the increase in electron-accepting ability of group I by 13.2 e as compared to TZ1, clearly suggesting the greater electron donation by $-NH_2$ group, which is also substituted on group II at ortho-position to –COOH group.

3.5 *First hyperpolarizability*

Optical nonlinearities in octupolar molecules are decided by the multidirectional CT, taking place in the different fragments of the molecule. The generalized Mulliken–Hush analysis confirms that the CT in excited state is necessary for a molecule to be optically non-linear. It is known that along with increasing the donor or acceptor strength, one should also observe the delocalization or localization of the two states for enriching hyperpolarizability [57,58]. The optimum hyperpolarizability can be obtained at an appropriate point, at which there is an appreciable overlap of the wave functions that define the two states [59]. It has been observed that to achieve high hyperpolarizability, it is necessary to obtain overlapping of HOMO and LUMO levels over the π-conjugated bridge in an organic push–pull system [60,61].

3.5a *Effect of functionals*: The effect of functionals like B3LYP, CAM-B3LYP, M062X, LC-WPBE, BHandHLYP and WB97XD on first hyperpolarizability (β) was evaluated by using 6-311G(d, p) basis set in gas phase, which were applied on B3LYP/6-311G(d, p) optimized geometries of the molecules in gas phase (supplementary table S8). The trend of variation of β from one molecule to another was similar in all the functionals and all the molecules maintained same order of 10^{-29} esu of β value in all the functionals.

The experimental first hyperpolarizability of the molecule TZ1 is reported as 1.6×10^{-29} esu by Ray *et al* [62]. The functional B3LYP slightly overestimated β, while CAM-B3LYP, M062X, BHandHLYP, LC-WPBE and WB97XD predicted β values are very close to the experimental value.

We followed CAM-B3LYP generated results (where β of TZ1 is 1.83×10^{-29} esu), since it presented satisfactory agreement of both absorption properties and β with their experimental ones.

3.5b *Effect of basis sets*: The results of the evaluation of influence of different basis sets (6-311G(d, p), 6-311+G(d, p) and 6-311++G(d, p)) on β is shown in supplementary table S9. From supplementary table S9, it can be noticed that β values slightly increase as we move from lower to higher basis sets; but molecules retained the same order of 10^{-29} esu of β in all basis sets. The experimental β of TZ1 is 1.6×10^{-29} esu [59]. The 6-311G(d, p), 6-311+G(d, p) and 6-311++G(d, p) basis sets predict β value to be 1.83×10^{-29}, 1.88×10^{-29} and 1.89×10^{-29} esu, respectively (supplementary table S9), which are all closer to experimental β. Hence, the calculations of β is carried out using 6-311G(d, p) basis set to reduce the time of computation and succeeding discussion on β follows the output generated by CAM-B3LYP/6-311G(d, p) method in gas phase.

The calculated first hyperpolarizabilities of the current series of molecules are presented in table 4. The trend of β for these molecules follows the order: TZ < TZ11 < TZ12 < TZ10 < TZ1 < TZ9 < TZ8 < TZ2 < TZ4 < TZ7 < TZ3 < TZ6 < TZ5.

The greater the electron-donating ability of a substituent, the higher will be the magnitudes of CT from donor end to acceptor end, which in turn boosts charge delocalization throughout molecule [39]. Hence, asymmetric charge distribution created in this way increases β as donor strength increases. The molecules TZ2, TZ3, TZ4, TZ5, TZ6 and TZ7 contain electron-donating substituents such as $-CH_3$,

Table 4. The first hyperpolarizabilities (β in 10^{-29} esu) of molecules from TZ to TZ12 calculated at CAM-B3LYP/6-311G(d, p) level.

Name	TZ	TZ1	TZ2	TZ3	TZ4	TZ5	TZ6	TZ7	TZ8	TZ9	TZ10	TZ11	TZ12
β	0.03	1.83	2.86	4.44	3.13	5.39	4.95	3.33	2.41	1.86	1.24	0.76	1.21

$-OCH_3$, three $-OCH_3$ groups, $-NH_2$, $-NHCOCH_3$ and –Cl, respectively.

The TZ5 molecule shows maximum first hyperpolarizability, because of the greater electron-donating effect of amine group. The molecules TZ6 and TZ3 achieve high first hyperpolarizability due to the electron-donating mesomeric effect of the substituted $-NHCOCH_3$ and $-OCH_3$ groups, respectively. The moderate electron donation by –Cl group in TZ7 contributes to the enhancement of its first hyperpolarizability. The electron-donating mesomeric effect and also the electron-withdrawing inductive effect of the three $-OCH_3$ groups substituted on each of the AR fragments of the molecule TZ4 has slightly diminished its β value as compared to TZ7. The lesser electron donation by $-CH_3$ groups has placed the molecule TZ2 in the lower range of first hyperpolarizability.

When there are electron-withdrawing substituents in a molecule; the electronic charge gets localized mainly on electron-withdrawing groups instead of delocalization throughout the molecule, which is unfavourable for increasing β values. Hence, though charge asymmetry is created; the absence of electron delocalization reduces β as the electron-withdrawing power of substituents increases.

The electron-withdrawing $-CN$ and $-CF_3$ groups on the molecules TZ8 and TZ9, respectively, have reduced their first hyperpolarizability as compared to TZ2. The electron-withdrawing nature of –F, $-NO_2$ and –COOH groups has reduced the first hyperpolarizability of the molecules TZ10, TZ11 and TZ12, respectively.

The molecule TZ1 bears the AR fragments, which contain the unsubstituted phenyl ring and hence, show the lower value of first hyperpolarizability. The unsubstituted s-triazine (TZ) shows the lowest first hyperpolarizability. These results point out the significance of choice of substitution, while designing the NLO materials.

The experimental β of standard molecule p-nitroaniline (PNA) is 1.69×10^{-29} esu [63]. Except TZ and TZ11, all other molecules exhibit good β values, which are comparable to PNA and can be explored for their applications in constructing NLO-based devices.

4. Conclusions

The linear and non-linear optical properties of some D–A type triazine derivatives were investigated focussing on the effect of varying substitution on the triazine core by DFT methods. The main findings of this work are: (a) the wavelength of maximum absorption gets redshifted as donor strength increases, (b) strong donors facilitate greater charge movement in molecule, (c) strong electron donors have a significant effect on the enhancement of first hyperpolarizability, (d) the TZ1, TZ2, TZ3, TZ4, TZ5, TZ6, TZ7, TZ8 and TZ9 molecules possess first hyperpolarizability of the order of 10^{-29} esu, which is comparable to that of standard molecule p-nitroaniline ($\beta = 1.69 \times 10^{-29}$ esu) [63] and can be prospective candidates for applications in non-linear optics. This structural design principle can be utilized to bring out lots of more efficient as well as novel NLO active molecules, with suitably altering the donor–acceptor characteristics.

Acknowledgements

CP thanks SERB, New Delhi, India, for financial support under Young Scientist Start-Up Research Grant (SB/FT/CS-101/2014). VVM acknowledges the Department of Science and Technology, Government of India, for financial support vide reference SR/WOS-A/CS-46/2017 under women scientist scheme to carry out this work.

Compliance with ethical standards

Conflict of interest The authors declare no competing financial interest.

References

[1] Schwarzer A, Saplinova T and Kroke E 2013 *Coord. Chem. Rev.* **257** 2032
[2] Bredas J L, Adant C, Tackx P, Persoons A and Pierce B M 1994 *Chem. Rev.* **94** 243
[3] Franken P A, Hill A E, Peters C W and Weinreich G 1961 *Phys. Rev. Lett.* **7** 118
[4] Williams D J 1984 *Angew. Chem. Int. Ed. Engl.* **23** 690
[5] Devi M S, Tharmaraj P, Sheela C D and Ebenezer R 2013 *J. Fluoresc.* **23** 399
[6] Thalladi V R, Brasselet S, Weiss H C, Blaser D, Katz A K, Carrell H L *et al* 1998 *J. Am. Chem. Soc.* **120** 2563
[7] Lu J, Xia P F, Lo P K, Tao Y and Wong M S 2006 *Chem. Mater.* **18** 6194
[8] Liu X K, Zheng C J, Xiao J, Ye J, Liu C L, Wang S D *et al* 2012 *Phys. Chem. Chem. Phys.* **14** 14255
[9] Sahu D, Tsai C H, Wei H Y, Ho K C, Chang F C and Chu C W 2012 *J. Mater. Chem.* **22** 7945
[10] Kwon J, Kim M K, Hong J P, Lee W, Noh S, Lee C *et al* 2010 *Org. Electron.* **11** 1288

[11] Kwon J, Kim M K, Hong J P, Lee W, Lee S and Hong J I 2013 *Bull. Korean Chem. Soc.* **34** 1355
[12] Thallpally P K, Chakraborty K, Carrel H L, Kotha S and Desiraju G R 2000 *Tetrahedron* **56** 6721
[13] Jetti R K R, Thallapally P K, Xue F, Mak T C W and Nangia A 2000 *Tetrahedron* **56** 6707
[14] Broder C K, Howard J A K, Keen D A, Wilson C C, Allen F H, Jetti R K R *et al* 2000 *Acta Cryst. B* **56** 1080
[15] Fabian L, Bombicz P, Czugler M, Kalman A, Weber E and Hecker M 1999 *Supramol. Chem.* **11** 151
[16] Munakata M, Wen M, Suenaga Y, Kuroda-Sowa T, Maekawa M and Anahata M 2001 *Polyhedron* **20** 2037
[17] Boraei A A A and El-Roudi O M 1996 *Can. J. Appl. Spec.* **41** 37
[18] Garcia A, Insuasty B, Herranz M A, Martinez-Alvarez R and Martin N 2009 *Org. Lett.* **11** 5398
[19] Shie J J and Fang J M 2007 *J. Org. Chem.* **72** 3141
[20] Wang M X and Yang H B 2004 *J. Am. Chem. Soc.* **126** 15412
[21] Saied H N, Khalil H H, Abdel M M, El-Wakil M H, Bekhit A A and Nabil K S 2019 *Bioorg. Chem.* **89** 103013
[22] Wu H, Hu R, Zeng B, Yang L, Chen T, Zheng W *et al* 2018 *RSC Adv.* **83** 7631
[23] Jin G F, Ban H S, Nakamura H and Lee J D 2018 *Molecules* **23** 2194
[24] Chouai A and Simanek E E 2008 *J. Org. Chem.* **73** 2357
[25] Steffensen M B and Simanek E E 2004 *Angew. Chem. Int. Ed.* **43** 5178
[26] Yu S Y, Mahmood J, Noh H J, Seo J M, Jung S M, Shin S H *et al* 2018 *Angew. Chem. Int. Ed.* **57** 8438
[27] Guo M, Wu J, Cador O, Lu J, Yin B, Le Guennic B *et al* 2018 *Inorg. Chem.* **57** 4534
[28] Zhang W, Yang D, Zhao J, Hou L, Sessler J L, Yang X J *et al* 2018 *J. Am. Chem. Soc.* **140** 5248
[29] Das P and Mandal S K 2018 *J. Mater. Chem. C* **6** 3288
[30] Dehghani Z, Dadfarnia S, Shabani A M H and Ehrampoush M H 2015 *Anal. Bioanal. Chem.* **2** 13
[31] Idzik K R, Frydel J, Beckert R, Ledwon P, Lapkowski M, Fasting C *et al* 2012 *Electrochim. Acta* **79** 154
[32] Ward J F 1965 *Rev. Mod. Phys.* **37** 1
[33] Oudar J L 1977 *J. Chem. Phys.* **67** 446
[34] Oudar J L and Le Person H 1975 *Opt. Commun.* **15** 258
[35] Le Cours S M, Guan H W, Di Magno S G, Wang C H and Therien M J 1996 *J. Am. Chem. Soc.* **118** 1497
[36] Oudar J L and Chemla D S 1977 *J. Chem. Phys.* **66** 2664
[37] Zyss J and Ledoux I 1994 *Chem. Rev.* **94** 77
[38] Meyers F, Marder S R, Pierce B M and Bredas J L 1994 *J. Am. Chem. Soc.* **116** 10703
[39] Gyoosoon P and Bong R C 2004 *J. Phys. Org. Chem.* **17** 169
[40] Zhu G W and Wu G S 2001 *J. Phys. Chem. A* **105** 9568
[41] Koeppen M, Beyer O, Wuttke S, Luening U and Stock N 2017 *Dalton Trans.* **46** 8658
[42] Becke A D 1993 *J. Chem. Phys.* **98** 5648
[43] Lee C, Yang W and Parr R G 1988 *Phys. Rev. B* **37** 785
[44] Frisch M J, Trucks G W, Schlegel H B, Scuseria G E, Robb M A, Cheeseman J R *et al* 2013 *Gaussian 09, Revision E.01* Gaussian, Inc.: Wallingford, CT
[45] Bredas J L, Meyers F, Pierce B M and Zyss J 1992 *J. Am. Chem. Soc.* **114** 10703
[46] Srinivas K, Prabhakar C, Sitha S, Bhanuprakash K and Jayathirtha R V 2014 *J. Mol. Struct.* **1075** 118
[47] Yanai T, Tew D P and Handy N C 2004 *Chem. Phys. Lett.* **393** 51
[48] Chai J D and Gordon M H 2008 *J. Chem. Phys.* **128** 084106
[49] Zhao Y and Truhlar D G 2008 *Theor. Chem. Acc.* **120** 215
[50] Vydrov O A and Scuseria G E 2006 *J. Chem. Phys.* **125** 234109
[51] Becke A D 1993 *J. Chem. Phys.* **98** 1372
[52] Llobera A, Saa J M and Peralta A 1985 *Synthesis* 95
[53] Stalin T and Rajendiran N 2006 *J. Photochem. Photobiol. A* **182** 137
[54] Huang W, Zhang X, Ma L H, Wang C J and Jiang Y B 2002 *Chem. Phys. Lett.* **352** 401
[55] Alexiou M S, Tychopoulos V, Ghorbanian S, Tyman J H P, Brown R G and Brittain P I 1990 *J. Chem. Soc. Perkin. Trans.* **25** 837
[56] Nemykin V N and Basu P 2001, 2003 *VMOdes Program, Revision A 7.1*, Department of Chemistry, Duquesne University, Pittsburgh, PA
[57] Marder S R, Kippelen B, Jen A K Y and Peyghammbarian N 1997 *Nature* **388** 845
[58] Zerner M C, Fabian W M F, Dworczak R, Kieslinger D W, Kroner G, Junek H *et al* 2000 *Int. J. Quantum. Chem.* **79** 253
[59] Kanis D R, Ratner M A and Marks T J 1994 *Chem. Rev.* **94** 195
[60] Yoshimura T 1989 *Phys. Rev. B* **40** 6292
[61] Yoshimura T 1989 *Appl. Phys. Lett.* **55** 534
[62] Ray P C and Das P K 1995 *Chem. Phys. Lett.* **244** 153
[63] Teng C C and Garito A F 1983 *Phys. Rev. B* **28** 6766